Experimental data for flow boiling of R450A in a horizontal tube

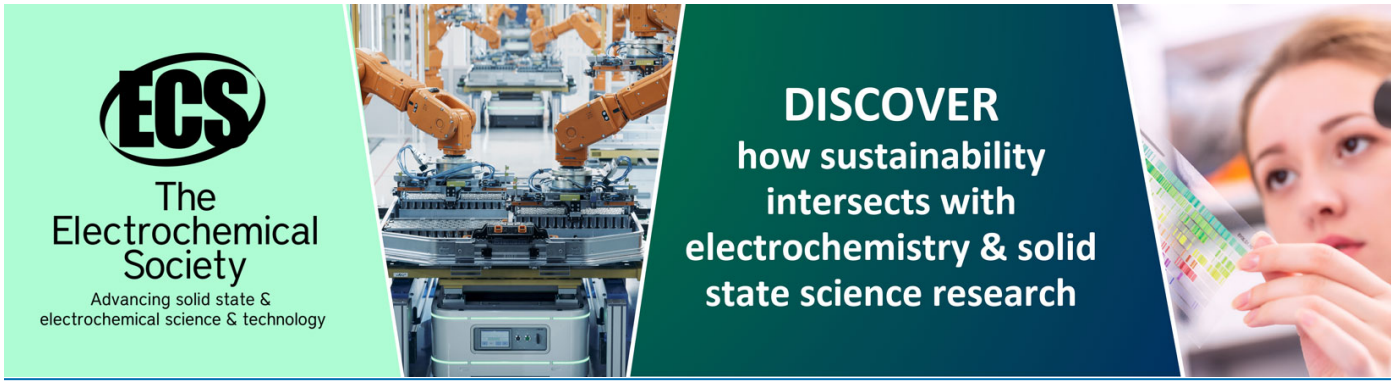

Experimental data for flow boiling of R450A in a horizontal tube

R Mastrullo[1], A W Mauro[1,*], A F Passarelli[1], I Viscardi[1] and L Viscito[1]

[1] Department of Industrial Engineering, Federico II University of Naples, P.le Tecchio 80, 80125 Naples, Italy

* Corresponding author: wmauro@unina.it

Abstract. According to the new European policies aimed at the replacement of highly-pollutant greenhouse gases refrigerants, the scientific community has focused on new synthetic environmentally friendly substances to be employed in vapor compression cycles for the refrigeration and the air conditioning fields.
On this regard, R450A is a new blend made up of R134a (42%) and R1234ze (58%), having a GWP equal to 604, and therefore represents an attractive solution as pure R134a substitute. In this paper, new flow boiling heat transfer and pressure drop data of R450A collected at the refrigeration lab of Federico II University of Naples are presented. The data refer to a horizontal stainless-steel tube having an internal diameter of 6.0 mm. The effects of mass flux (from 150 to 400 kg $m^{-2}s^{-1}$), heat flux (from 10 to 20 kW m^{-2}) and saturation temperature (from 30 to 50 °C) are presented and discussed, together with the assessment of the most quoted two-phase heat transfer and pressure drop prediction methods.

1. Introduction

Refrigeration and air conditioning systems are an essential part of modern life, providing cool air in homes, offices, vehicles, and many other applications. However, the use of halogenated fluids in vapor compressionsystems has provided a considerable contribution to the release of greenhouse gases in the atmosphere [1] [2] and therefore tothe undesired rise of the Earth temperature. In fact, most of the synthetic refrigerants present a high Global Warming Potential (GWP), and thus act as pollutant gases in case of accidental leakages [3] or during the plant dismission procedure. So far, the hydro-fluoro-carbon (HFC) R134a is the most common fluid in medium-temperature applications of both developed and developing countries. Its GWP is about 1480 [4] and is already banned in several fields according to the new European Regulations.Among possible substitutes, R450A is a blend of two refrigerants (mass fraction 42%/58% of R134a/R1234ze(E)), with a considerably lower GWP of 604 [4], non-toxic and non-flammable. It can be considered as a direct drop-in replacement of R134a [5] in existing commercial and industrial medium and high temperature refrigeration equipment that uses positive displacement compressors and direct expansion systems. It can also be suitable for heat pumps, vending machines, drink dispensers, centrifugal air and water chillers, and for replacing R134a in medium-temperature circuits of two-stage hybrid cascade systems with CO_2.

The rising interest towards this blend is testified by numerous scientific publications related to the performance comparison of several systems employing R450A as possible R134a substitute. Mota-

Babiloni et al. [6,7] tested R450A in a vapor compression plant equipped with a variable compressor and R134a as original working fluid. They found that R450A could lead to higher Coefficient of Performance (COP) values, lower discharge temperatures and lower pressure drop for the internal heat exchanger. Similar results were obtained by Makhnatch et al. [8] in a small refrigeration unit, reporting only a slight reduction in the cooling capacity when employing R450A. The same research group [9] experimentally investigated the use of R134a and alternative fluids in operating conditions typical of countries with high ambient temperatures, finding a lower performance of R450A with respect to both R134aand R513A. For different applications, Gataric and Lorbek [10] tested R450A in household heat pump tumble dryers and Molinaroli et al. [11] in a water-to-water heat pump, with similar outcomes related to the energy consumption and efficiency (not much different from R134a) and heating capacity (slightly reduced because of the lower condensation pressure with respect to R134a). Several numerical approachesincluding Artificial Intelligence have also been followed to investigate the possible use of R450A in refrigeration systems (Belman-Flores et al., 2017 and Zendehboudi et al., 2019) [12] [13] and in waste heat-solar driven ejector heat pumps for simultaneous heating and cooling (Al-Sayyab et al., 2021) [14], all with encouragingand positive outcomes.

Besides system analyses, the literature review presents fewer examples related to the two-phase thermal and hydraulic characteristics of R450A, and most of them are related to condensation heat transfer. Jacob et al. [15] conducted experiments on R450A condensing in a 4.7 mm tube, using a novel distributed temperature sensor. More recently, Azzolin et al. [16] experimented flow condensation of R450A in smalltube channels having internal diameters of 0.96 mm and 3.38 mm, providing also flow visualization results. Diani et al. [17] tested the new blend in a 7 mm outer diameter microfin tube during flow condensation, highlighting the significant effect of mass velocity, especially for in the low vapor quality region. A comparisonwith R134a was proposed by Morrow and Derby [18], that experimented condensation heat transfer in a set of 7 parallel minitubes with a diameter of 0.95 mm. They found that the heat transfer coefficients of R450A could be up to 25% lower than the ones obtained for the reference fluid. To the best of our knowledge,the only work in literature concerning flow boiling heat transfer of R450A is that of Kedzierski and Kang [19] in a microfin tube. The authors found that both two-phase heat transfer coefficient and pressure drop were15% lower than those obtained for R134a in the same conditions and proposed a correlation to improve thestatistics of their assessment.

Since no studies are aimed at the investigation of flow boiling characteristics of R450A in smooth conventional channels, more data on these configurations could be useful to assess the existing correlation and to correctly design evaporators in vapor compression systems. For this reason, the present study explores thermal and hydraulic characteristics of R450A in a horizontal stainless-steel tube having an internal diameter of 6.0 mm. The experiments are aimed to evaluate the heat transfer coefficient and the frictional pressure gradient in different operating conditions in terms of mass flux, imposed heat flux, saturation temperature and vapor quality, finally proposing an assessment with the most quoted prediction methods.

2. Experimental apparatus

2.1. Refrigerant loop and test tube

Figure 1 shows a schematic view of the experimental plan. The refrigerant in sub-cooled condition flows thorough a magnetic gear pump and the flow rate is measured by a Coriolis flow meter before the preheating section. The latter is made up of a copper tube where the heatis provided by four fiberglass heating tapes.The applied heat at the preheater section is modulated through a solid-state relay to obtain a specific local vapor quality at the inlet of the test section. The following plate heat exchanger and tube-in-tube heat exchanger work respectively as condenser and sub-cooler before the pump suction head that closes the loop. Several throttling valves are positioned on the liquid and vapor lines, respectively, and a bypass loop is placed at the pump outlet to have multiple mass flow rate control options. The coolant is demineralized water, with its temperature set and remotely controlled by a thermostatic bath.

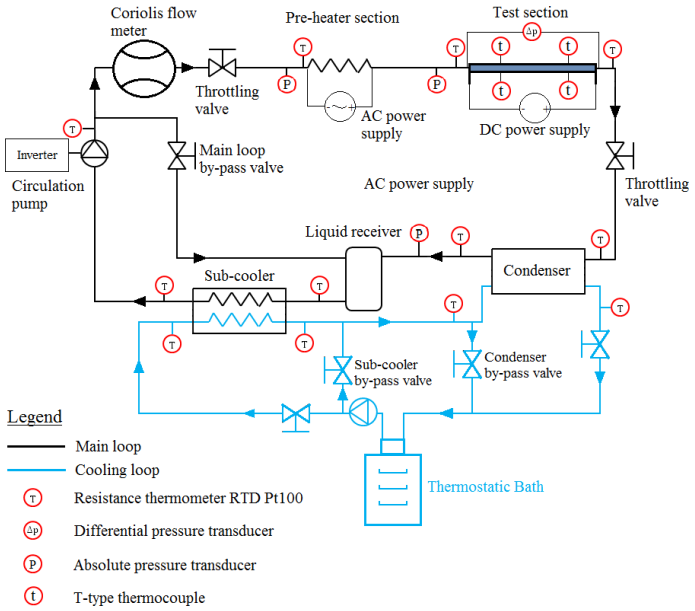

Figure 1. Experimental apparatus.

The test section employed for the present experimental campaign is a smooth, horizontal, circular stainless steel (AISI SS316) tube with an internal diameter of 6.0±0.05 mm and an outer diameter of 8.0±0.05 mm. The heat flux is obtained through Joule effect provided by a modulable DC power supply unit with 193.7±0.79 mm representing the total measured heated length (see points A and E in Figure 2). Two pressure taps are placed at 237.5±0.91 mm from point A and are useful for the inlet pressure and pressure drop measurements. For the evaluation of the local heat transfer coefficient, point C (see Figure 2) is placed at 146.7 ±0.64 mm from the inlet section. More details are available in some authors' previous works [20, 21, 22] (Lillo et al., 2018, Arcasi et al., 2021, 2022).

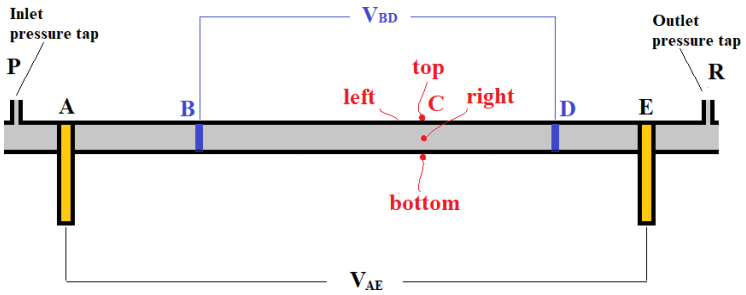

Figure 2. Test tube.

2.2. Measurement instrumentation

Both the main and secondary loops are equipped with several resistance thermometers (RTDs) having an overall uncertainty of ±0.180 °C, able to measure the working and cooling fluid temperatures. Four T-type thermocouples are instead placed at the measurement point C and evaluate the outer wall temperature forthe calculation of the two-phase heat transfer coefficient. Following a dedicated in-situ calibration that includes two high-accuracy resistance thermometer (one placed on the tube and the other placed in the environment for the compensation of the cold junction temperature) and adiabatic tests, the overalluncertainty that also includes the residual errors of the calibration curve is estimated as ±0.1 °C.

The test section inlet pressure is obtained through an absolute pressure transducer having a measuring range of 0-35 bar and an overall uncertainty of ±0.5% of the read value, whereas the pressure drop is estimated with a differential pressure transducer, carrying an instrumental uncertainty of ±0.06 kPa.

A Coriolis flow meter provides the value of the mass flow rate with a maximum uncertainty of ±1% of the measurement. For the preheating section, the AC voltage (100 mV-500 V) and current (1 mA-16 A) are separately measured, and the total uncertainty of the estimated ohmic electrical power is ±1.0% of the reading, as provided by the manufacturer. Finally, the DC ohmic power for the test section is obtained through separate measurements of voltage (transducer within 0-5 V and an uncertainty of ±0.03% of the reading) and current (directly measured by the DC power unit within 0-300 A and an uncertainty of ±1.0%).

3. Method

3.1. Data reduction process

All the calculations have been implemented in MATLAB [23] environment, and the thermodynamic and transport properties, when not differently detailed, are obtained through the software Refprop 10.1 [24]. The local heat transfer coefficient is calculated according to the Newton law, Eq. (1):

$$h = \frac{q}{T_{wall} - T_{sat}} \tag{1}$$

The inner T_{wall} is obtained from the outer wall temperature T_{th} by considering the analytical solution to the heat transfer phenomenon with the hypothesis of 1-D heat flux in the radial direction, uniform heat generation inside the tube, as shown in Equation (2):

$$T_{wall} = T_{th} + \frac{V_{BD} \cdot I}{4\pi\lambda_{tube}\overline{BD}} \cdot \left[\left(\frac{D}{d}\right)^2 \cdot \left(1 - ln\left(\left(\frac{D}{d}\right)^2\right)\right) - 1\right] \cdot \left[\left(\frac{D}{d}\right)^2 - 1\right]^{-1} \tag{2}$$

T_{sat} is instead the local saturation temperature in the measurement point, obtained as a function of the local pressure and enthalpy, by interpolating the saturation curve experimentally obtained with adiabatic experiments, in which the temperature is estimated with a resistance thermometer. The local heat flux is instead the measurement of an electric quantity, as shown in Equation (3):

$$q = \frac{V_{BD} \cdot I}{\pi d \overline{BD}} \tag{3}$$

To keep into account the non-negligible glide of the tested mixture [25] (Mauro et al., 2020), the local vapor quality at the measurement point is obtained as a function of both saturation temperature and local specific enthalpy. This latter value is the result of an energy balance over the preheating and the test section up to the measurement point, as shown in Equation (4).

$$i_c = i_{in,preh} + \frac{\dot{Q}_{preh}}{\dot{m}} + \frac{\dot{Q}_{TS} \cdot \left(\frac{\overline{AC}}{\overline{AE}}\right)}{\dot{m}} \tag{4}$$

The frictional pressure drop has been calculated as the measured pressure gradient divided by the distance between the two pressure ports (see points P and R in Figure 2). In fact, all pressure drop values presented in this work are obtained at adiabatic conditions and with a horizontal configuration; therefore geodetical and momentum contributions are null.

3.2. Uncertainty analysis and validation

The law of propagation of error [26] was used to estimate the combined uncertainty of all measured and derived parameters, by also using a coverage factor of 2 to ensure a confidence level higher than 95%. The average uncertainty related to the heat transfer coefficient and pressure drop is ± 16.87% and ± 14.57%, respectively.

Liquid single-phase experiments by using refrigerant R134a were carried-out to evaluate the correct insulation and the proper functioning of the measurement instrumentation. The electrical power in the preheater and test section was compared to the heat absorbed by the sub-cooled refrigerant, with good results. Also, the liquid single-phase heat transfer coefficients were evaluated and compared to benchmark correlations. Further information on the validation procedure can be obtained from previous works with the same test facility [27, 28] (Lillo et al., 2018b, Mastrullo et al., 2017).

4. Results

R450A is the working fluid employed for the convective boiling experiments. Mass fluxes of 150 and 400 kg $m^{-2}s^{-1}$, heat fluxes from 10 to 20 kW m^{-2} and bubble saturation temperatures from 30 to 50 °C have been investigated and the effect of their variation on the local heat transfer coefficients and pressure drop values(obtained at adiabatic conditions) is discussed in the following diagrams.

4.1. Heat transfer coefficient

The effect of the operating conditions on the R450A flow boiling heat transfer coefficients is shown in Figure 3a-c.

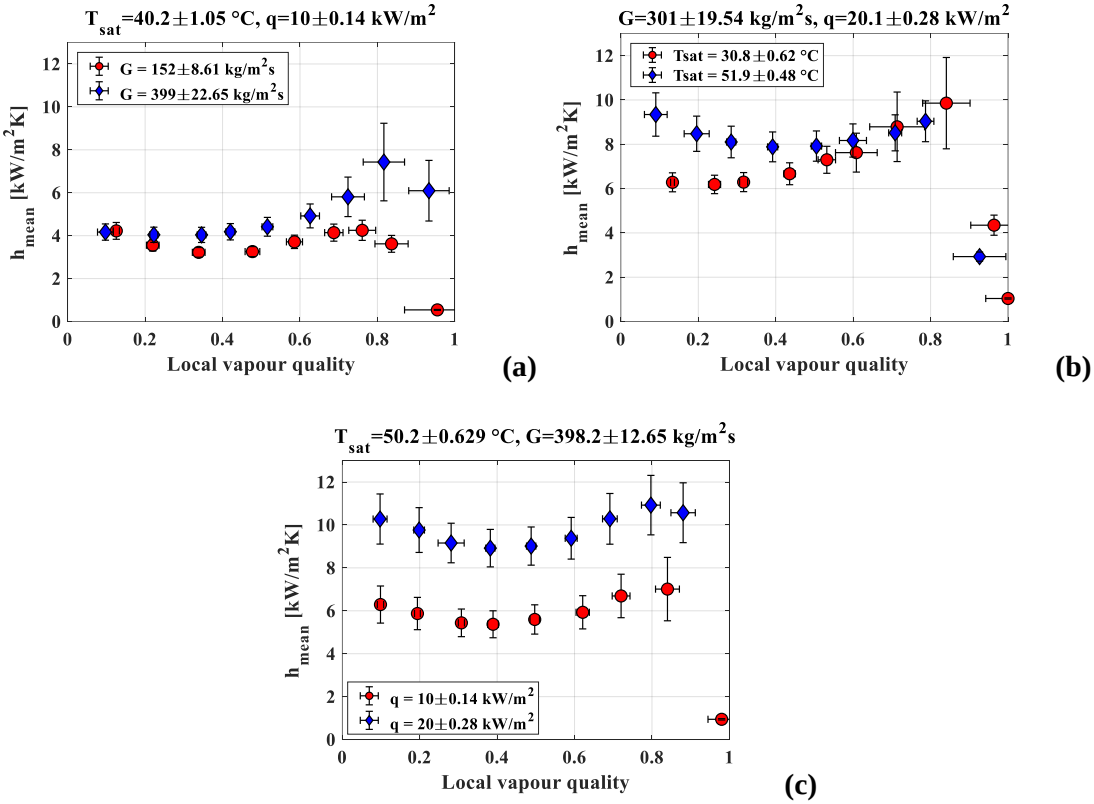

Figure 3. Effect of the operating conditions on the R450A flow boiling heat transfer coefficient. (a) Effect of mass velocity; (b) Effect of bubble saturation temperature; (c) Effect of the heat flux.

As regards the influence of the mass flux (see Figure 3a), the increasing trend with vapor quality is found to be representative of the heat transfer coefficient behaviour only for high mass velocities. In case of G equalto 150 kg $m^{-2}s^{-1}$, instead, the trend is somehow decreasing and may imply a possible early dry-out phenomenon or a stratified flow regime. The local peripheral heat transfer coefficient values validate this assumption, since it was observed a sudden drop of the top heat transfer coefficient already at low vapor qualities. The effect of the saturation temperature is shown in Figure 3b. The increase of the

system pressureleads to lower heat transfer coefficients for high vapor qualities, in which the convective contribution plays a major role. In fact, the increase of the reduced pressure lowers the difference betweenliquid and vapor phase densities and therefore decreases the shear stress at the interface with a consequent penalization on the convective heat transfer contribution. At lower vapor qualities, instead, the heat transfer coefficient increases with the saturation temperature, implying a significant nucleate boiling contribution, that is enhanced with reducing surface tension for higher system pressures. Finally, the effect of the imposed heat flux is shownin Figure 3c, with a significant increase of the boiling heat transfer coefficient (up to 200%) whenpassing from 10 to 20 kW m^{-2}. This implies that the nucleate boiling contribution is preponderant for such conditions and the increase of the heat flux enhances the nucleation sites activity, with more bubble per unit time at the wall.

The experimental data have been compared to some well-known correlations to test their accuracy within the present range of operating conditions. The best results have been found with the prediction methods of Li and Wu (2010) [29] and Del Col (2010) [30], as shown in Figure 4a-b, respectively. The first provides a Mean Absolute Percentage Error (MAPE) of 26.50% and a Mean Relative Percentage Error of 0.17%.The latter provides a MAPE of 20.36% and a MRPE of -9.89%. The prediction method of Wojtan et al. [19] shows better fitting of the experimental data for high values of vapour quality, while for low values of vapour quality the method does not work properly. Other methods were also tested with even larger errors, thus being excluded from this graphical comparison.

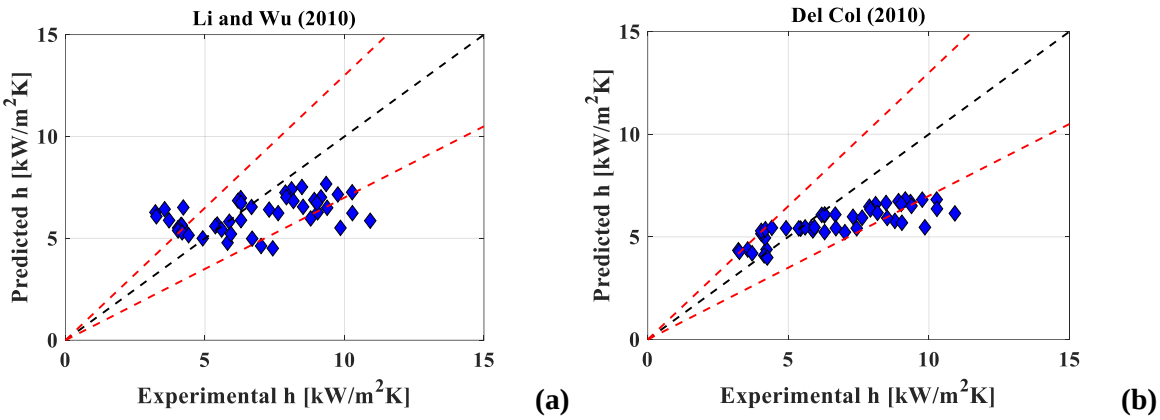

Figure 4. Predicted vs experimental heat transfer coefficient. (a) Li and Wu (2010) correlation; (b) Del Col (2010) correlation.

4.2. Pressure drop

All pressure drop experiments have been obtained within the same range of parameters used for the heat transfer coefficient tests, except for the adiabatic conditions maintained for such analysis. The effect of the mass flux and of the bubble saturation temperature on the frictional pressure gradient is provided in Figure 5a-b. Larger pressure drop values are obtained, as expected, for higher values of the mass velocity. In fact, its increase leads to higher flow velocities and therefore higher friction. On the contrary, the flow reduces itsspeed with the increase of the saturation temperature, due to a progressively higher vapor density when approaching the critical point.

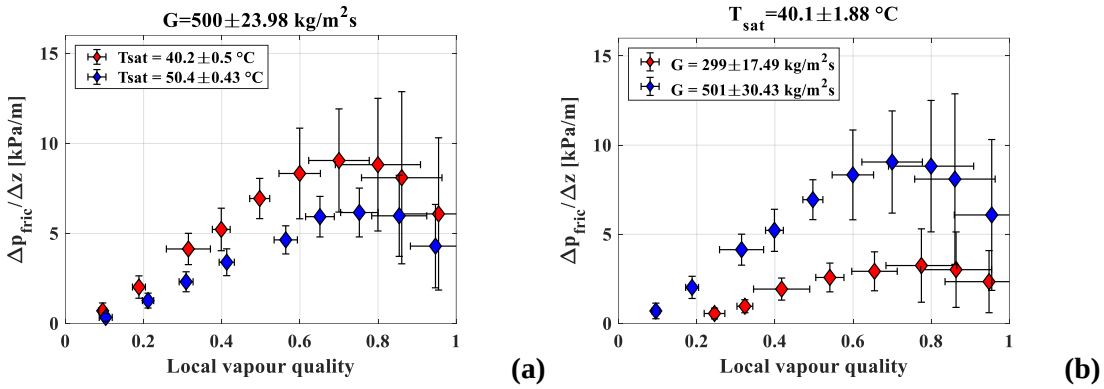

Figure 5. Effect of the operating conditions on the R450A two-phase pressure drop. (a) Effect of mass velocity; (b) Effect of bubble saturation temperature.

The assessment of the two-phase frictional pressure gradient prediction methods is graphically shown in Figure 6a-b for the correlations of Cicchitti (1960) [31] and Müller-Steinhagen and Heck (1986) [32], respectively. The best accuracy was obtained with the homogeneous flux model of Cicchitti [31] having a MAPE of 33.15% and a MRPE of 8.88%. Similarly, the Müller-Steinhagen and Heck correlation (1986) [32] provides a MAPE of 29.92% and a MRPE of 21.69%.

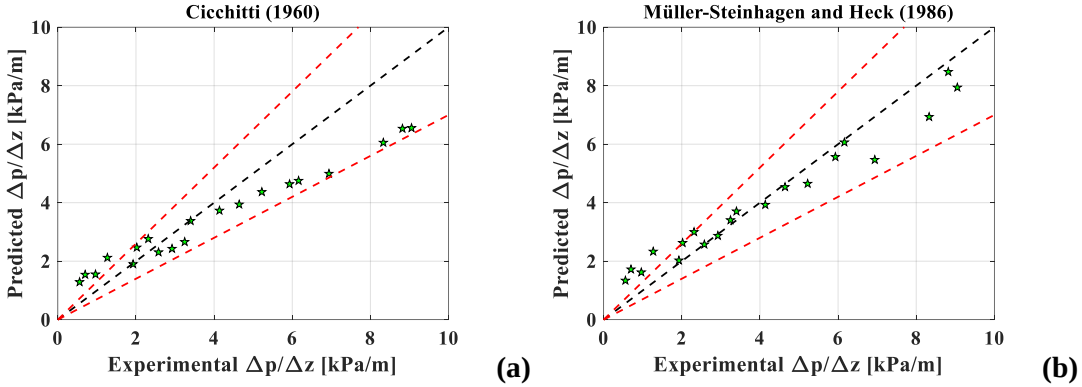

Figure 6. Predicted vs experimental pressure drops. (a) Cicchitti's model (1960); (b) Müller-Steinhagen and Heck (1986) correlation.

5. Conclusions

Two-phase flow boiling heat transfer coefficient and pressure drop data of refrigerant R450A have been collected in this paper. The effect of the operating conditions imposed has been analyzed and the assessmentof some correlations has been performed. The main outcomes are listed as follows:

- The vapor quality has a positive effect on the boiling heat transfer coefficient up to the dry-out condition, especially with high values of the mass velocity. For low mass fluxes, instead (150 $kgm^{-2}s^{-1}$), an early dry-out can be detected right after the onset of boiling. The saturation temperature has a negative effect on the heat transfer coefficient, due to a reduction of the flow velocity, whereas the heat flux significantly enhances the heat transfer performance, thus showing a non-negligible nucleate boiling contribution.
- The correlation of Del Col et al. [30] best fits the heat transfer coefficient experimental data, with a MAPE of 26.50% and a MRPE of -0.17%.
- The frictional pressure gradients at adiabatic conditions are increased with increasing mass flux and decreasing saturation temperature. The model of Müller-Steinhagen and Heck works

best with the present database with a MAPE of 29.92% and a MRPE of 21.69%.

6. References

[1] Abas N, Kalair A R, Khan N, Haider A, Saleem Z, Saleem M S 2018 *Renew. Sustain. Energy Rev*. **90** 557–569
[2] Choi S, Oh J, Hwang Y, Lee H 2017 *Appl. Therm. En.* **120** 88–98
[3] Pelella F, Viscito L, Mauro A W 2022 *Energy Conversion and Management* **260** 115646
[4] Metz B, Davidson O, Bosch P, Dave R, Meyer L 2007 *Fourth Assessment Report of the Intergovernmental Panel on Climate Change*
[5] Khan M, Wen J, Shakoori M.A, Tao, W 2022 *J. of Molecular Liquids* **353** 118795
[6] Mota-Babiloni A, Navarro Esbrì, J, Barragàn-Cervera A, Moles F, Peris B 2015 *Int. J. Refrigeration* **51** 52-58
[7] Mota-Babiloni A, Navarro Esbrì J, Barragàn-Cervera A, Moles F, Peris, B 2015 *Energy* **90** 1636-1644
[8] Makhnatch P, Mota-Babiloni A, Kodabandeh R, 2017 *Int. J. Refrigeration* **84** 26-35
[9] Makhnatch P, Mota-Babiloni A, Lopez-Belchi A, Kodabandeh R *Energy* **166** 223-235
[10] Gataric P, Lorbek L 2021 *Int. J. Refrig.* **128** 22–33
[11] Molinaroli L., Lucchini A, Colombo L P M 2021 *Int. J. Refrig.* **135** 139–147
[12] Belman-Flores J M , Mota-Babiloni A, Ledesma S, Makhnatch P 2017 *Applied Thermal Engineering* **127** 996-1004
[13] Zendehboudi A, Mota-Babiloni A, Makhnatch P, Saidur R, Sait S M 2019 *Int. J. Refrigeration* **100** 141-155
[14] Al-Sayyab A K S, Mota-Babiloni A, Navarro-Esbrì J 2021 *Energy Conversion and Management* **228** 113703
[15] Jacob T A, Matty E P, Fronk B M 2019 *Int. J. Refrigeration* **103** 274-286
[16] Azzolin M, Berto A, Bortolin S, Del Col D 2022 *Int J. Refrigeration* **137** 153-165
[17] Diani A, Liu Y, Wen J, Rossetto L 2022 *Int. J. Heat Mass Transfer* **196** 123260
[18] Morrow J A, Derby M M 2022 *Int. J. Heat Mass Transfer* **192** 122894
[19] Wojtan L, Ursenbacher T, Thome J R 2005 *Int. J. Refrigeration* **48** 2970-2985
[20] Lillo G, Mastrullo R, Mauro A W, Viscito L 2018 *Int. J. Heat Mass Transfer* **126** 1236-1252
[21] Arcasi A, Mastrullo R, Mauro A W, Viscito L, 2021 *Int. J. Heat Mass Transfer* **164** 120604
[22] Arcasi A, Mauro A W, Napoli G, Viscito L 2022 *Int. J. Heat Mass Transfer* **188** 122599
[23] MATLAB 2019a Release *Mathworks*
[24] Lemmon E W, Mc Linden M O, Huber M L 2009 *REFPROP NIST* Database **23**
[25] Mauro A W, Napoli G, Pelella F, Viscito L 2020 *Int. J. Refrigeration* **119** 195-205
[26] Moffat J R 1985 *J. Fluids Eng.* **107** 173-178
[27] Lillo G, Mastrullo R, Mauro A W, Viscito L 2018 *Energy Procedia* **148**,1034- 1041.
[28] Mastrullo R, Mauro A W, Viscito L 2017 *Journal of Physics: Conference Series* **923** 012015
[29] Li W, Wu Z 2010 *Int. J. Heat Mass Transfer* **53** 1967-1976
[30] Del Col D 2010 *Exp. Therm. Fluid Sci.* **34** 234-245
[31] Cicchitti A, Lombardi C, Silvestri M, Soldaini G, Zavalluilli R 1960 *Energia Nucleare 7* 407-425
[32] Müller-Steinhagen H, Heck K, 1986 *Chem. Eng. Proceedings* **20** 297–308